Liquid Crystals

ISSN: (Print) (Online) Journal homepage: https://www.tandfonline.com/loi/tlct20

Influence of multifluorophenyloxy terminus on the mesomorphism of the alkoxy and alkyl cyanobiphenyl compounds in search of new ambient nematic liquid crystals and mixtures

Kunlun Wang, Mohammad S. Rahman, Tibor Szilvási, Jake I. Gold, Nanqi Bao, Huaizhe Yu, Nicholas L. Abbott, Manos Mavrikakis & Robert J. Twieg

To cite this article: Kunlun Wang, Mohammad S. Rahman, Tibor Szilvási, Jake I. Gold, Nanqi Bao, Huaizhe Yu, Nicholas L. Abbott, Manos Mavrikakis & Robert J. Twieg (2021) Influence of multifluorophenyloxy terminus on the mesomorphism of the alkoxy and alkyl cyanobiphenyl compounds in search of new ambient nematic liquid crystals and mixtures, Liquid Crystals, 48:5, 672-688, DOI: 10.1080/02678292.2020.1810792

To link to this article: https://doi.org/10.1080/02678292.2020.1810792

LIQUID CRYSTALS
2021, VOL. 48, NO. 5, 672–688
https://doi.org/10.1080/02678292.2020.1810792

Taylor & Francis
Taylor & Francis Group

Influence of multifluorophenyloxy terminus on the mesomorphism of the alkoxy and alkyl cyanobiphenyl compounds in search of new ambient nematic liquid crystals and mixtures

Kunlun Wang[a,b], Mohammad S. Rahman[a], Tibor Szilvási[c], Jake I. Gold[c], Nanqi Bao[d], Huaizhe Yu[d], Nicholas L. Abbott[d], Manos Mavrikakis[c] and Robert J. Twieg[a]

[a]Department of Chemistry and Biochemistry, Kent State University, Kent, OH, USA; [b]School of Materials Science and Engineering, Zhengzhou University, Zhengzhou, Henan, China; [c]Department of Chemical and Biological Engineering, University of Wisconsin-Madison, Madison, WI, USA; [d]Department of Chemical and Biomolecular Engineering, Cornell University, Ithaca, NY, USA

ABSTRACT

A series of cyanobiphenyl (CB) and cyano-p-terphenyl (CT) derivatives containing a variety of highly fluorinated aryloxyl termini and different connecting bridges were efficiently synthesized via aromatic nucleophilic substitution (S_NAr) and their mesogenic properties described. Comparison with the non-fluorinated analogues indicates that the terminal multifluoroaryloxy group generally decreases the crystal to nematic phase transistion temperature and enhances the supercooling of these mesogens. Furthermore, several binary LC mixtures formed by the multifluoroaryloxy tail-terminated compounds were found exhibiting promising wide room temperature nematic phases ranges comparable to the commercial quaternary mixture E7. Our binding free energy (G_{BE}) calculations predict that the fluorinated aryloxy terminated molecules tend to assume homeotropic orientation on $Al(ClO_4)_3$ and $Ni(ClO_4)_2$ metal salt decorated surfaces, which is consistent with the observed anchoring behavior. As such, these materials are promising candidates for chemoresponsive sensor devices which display a rapid response to a variety of analytes.

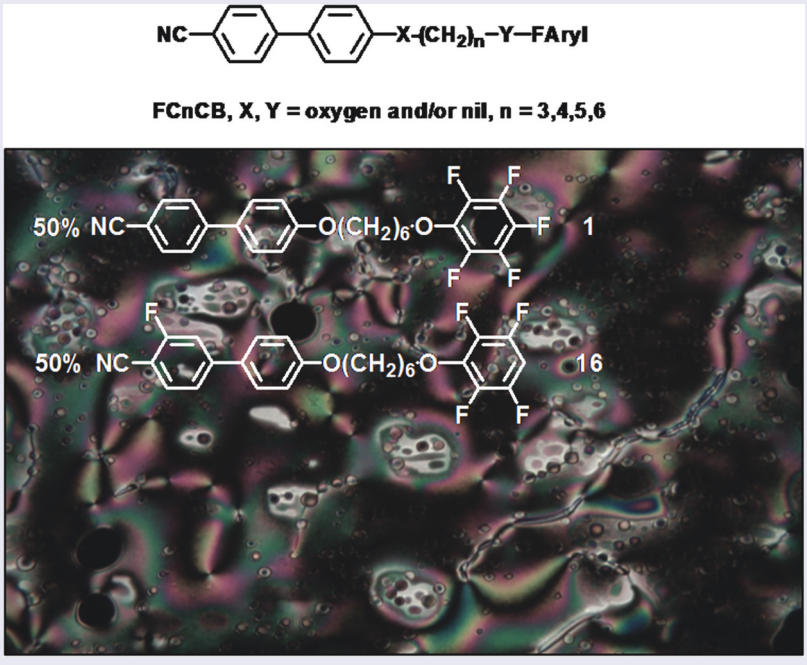

ARTICLE HISTORY
Received 03 July 2020
Accepted 12 August 2020

KEYWORDS
cyanobiphenyl; aromatic nucleophilic substitution; nematic phase; homeotropic anchoring; chemoresponsive sensor

1. Introduction

Liquid crystals (LC) possess a variety of interesting physical properties and continuous studies have been done on the design and synthesis of novel mesogens that exhibit improved properties in order to fulfill needs for enhanced performance. The mesogens of the K series

CONTACT Robert J. Twieg rtwieg@kent.edu; emavrikakis@wisc.edu
Supplemental data for this article can be accessed here

4-alkyl-4′-cyanobiphenyls (nCB) and the M series 4-alkoxy-4′-cyanobiphenyls (nOCB) have found wide applications in many types of devices including liquid crystal displays (LCD) [1]. Structural modifications such as substitution of both aromatic and aliphatic hydrogens by other atoms (halogen atoms for example) and/or functional groups have a dramatic influence on the phase behaviour of the K and M series LCs [2–6].

More recently, in our pursuit of novel room temperature nematogens for chemoresponsive sensors, the functionalization of the terminus of the flexible tail has been systematically examined for CB and OCB systems and some promising outcomes are revealed Figure 1 [7–9]. For example, a single fluorine atom installed in lieu of a hydrogen atom at the end of the flexible chain can suppress the formation of a smectic phase that is typical in both the K and M series with longer chains [8]. In addition, a cyano terminus on flexible tail enhances the supercooling properties, which has been found to be useful to achieve room temperature nematic mixtures.

After recognition that the mesogenicity of the parent rod-like LC molecules was considerably influenced by a terminal group on the flexible chain, our investigation has now proceeded to a larger terminus—a phenyl ring. In our previous work on cyano-terminated LCs [9], the CB compound with a pentafluorophenyloxy end group, **PFC6OCB** (Scheme 1), attracted our attention. This substance was reported by T. Itahara [10] to have a near ambient temperature nematic phase and while working with this material we have found that it also possesses significant supercooling. We have now utilised this substance to prepare wide temperature range binary nematic mixtures by combining it with other terminal functionalised LCs [9]. There are a few examples of mesogens with non-fluorinated [11] and monofluorinated [10,12] phenyloxy terminus known so far. Some CB compounds with 2,4-dimethylphenyloxy terminus were found exhibiting monotropic mesophases [13]. Stable nematic phases have been found for some non-fluorinated 4-vinylphenyloxy terminated derivatives, which were prepared as precursors for photopolymerisation [14,15]. Notably, if the size of the phenoxy tail terminus is expanded to a 4-phenylphenyloxy, then such systems become structurally similar to cyanobiphenyl dimers [16–20] some of which are

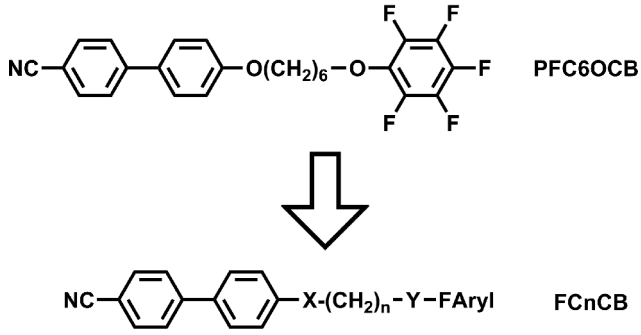

Scheme 1.

now understood to possess the interesting twist bend nematic phase.

In this work, using alcohol tail-terminated synthetic intermediates from our previous work [7–9] and commercially available highly fluorinated aromatic precursors, a variety of multifluoroaryloxy tail-terminated CBs and cyano-*p*-terphenyls (CT) have been obtained with simple but versatile chemistry as shown in Table 1, 2, 3, 4 and 5. Structural variations including differing the number of carbon atoms in the bridge, modifying the number and location of ether linkages in the bridge as well as selective fluorination of the rigid core have also been performed in order to further tune the thermal behaviour of the mesogens. Promising ambient nematic LC mixtures have been achieved from these molecules (Scheme 1). Our pursuit of room temperature cyano-terminated mesogens is motivated by their applications in sensor applications [21,22]. Based on our calculations of binding free energy (G_{BE}), we predict that the fluorinated aryloxy terminated molecules tend to assume homeotropic orientation on $Al(ClO_4)_3$, $Ga(ClO_4)_3$, and $Ni(ClO_4)_2$ metal salt surfaces, which is consistent with the observed anchoring behaviour on $Al(ClO_4)_3$ and $Ni(ClO_4)_2$ decorated surfaces. These new materials are under examination for anchoring transition application.

2. Experimental section

Commercial-grade solvents were used without further purification. $PdCl_2$ was bought from Pressure Chemical (Pittsburgh, PA). Palladium on carbon (5%),

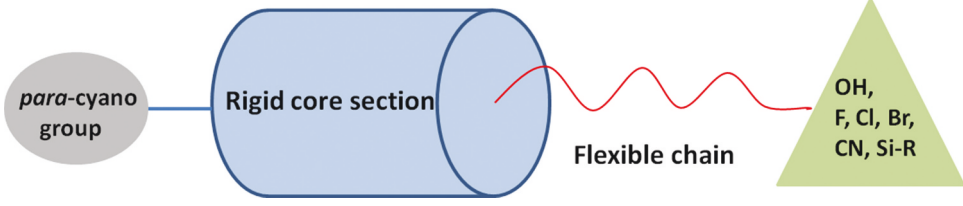

Figure 1. (Colour online) Preliminary examination of terminal functionalised derivatives of cyanobiphenyls (CB) and cyanoterphenyls (CT). R = alkyl group, etc.

Table 1. Phase behaviour of fluoroaryloxy terminated C6OCB derivatives **1**–**12** and non-fluorinated derivative **25**. (a. with 20% ortho adduct detected by NMR and the phase sequence was obtained for the mixture; b. with 17% ortho adduct detected by NMR and the phase sequence was obtained for the mixture; for other cases, only the para adduct was obtained and thermal behaviour examined. c. The nematic to crystal transition was found in the next cycle in DSC experiment.).

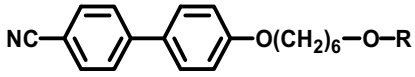

#	R	Phase behaviour (°C)
1 PFC6OCB [10]	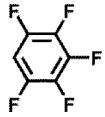	K 30.3 N 49.8 I 47.7 N – 35.7 K
2	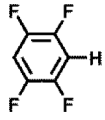	K 72.5 I 63.7 N 41.2 K
3		K 68.8 I 64.5 N 23.0 K [a]
4	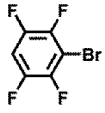	K 94 I 66.5 N 64 K[b]
5	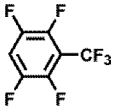	K 72.9 I 50 SmA 45 K
6	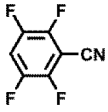	K 111.9 I 62.9 N 29.6 K
7	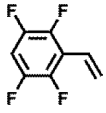	K 69.2 N 94.6 I 93.0 N 50.8 K
8	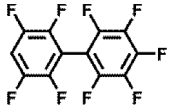	K 93.8 I 72.2 N 63.5 SmA 49 K
9	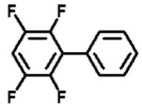	K 122.8 I 98.8 N 41.5 K
10	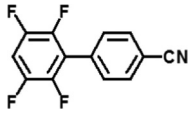	K 162 I 160 N 119 K
11	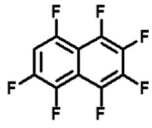	K 102.4 I 96.8 N 61.0 K_1 44.9 K_2
12	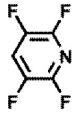	K 39.5 I 9.7 N 11.0 K[c]
25 PHC6OCB		K 103 I 85 K

diisopropylamine, ether and copper iodide were purchased from Acros. The precursor 4′-cyano-4-iodobiphenyl was prepared using a literature method [23]. The poisoned catalyst required for preferential alkyne reduction in the presence of a nitrile was also prepared using a literature method [24]. Triphenylphosphine and ethylenediamine were bought from Sigma-Aldrich. The pentafluoropyridine, pentafluorobenzonitrile, hexafluorobenzene, bromopentafluorobenzene chloropentafluorobenzene and pentafluorostyrene were purchased from Oakwood Products (Columbia, SC). The decafluorobiphenyl and pentafluorobenzene were purchased from Matrix Scientific (Columbia, SC). The terminal hydroxyacetylenes were purchased from GFS Organic Chemicals (Columbus, OH). The compressed hydrogen was bought from Linde Gas. Sythesis of all precursors can be accessed in supplemental information. The products were purified by column chromatography using silica gel (60–120 mesh) and/or by recrystallisation from analytical grade solvents.

Polarised optical microscopy (POM): Nikon ECLIPSE E600 Microscope & SPOT^{TM} idea COMS and Mettler Toledo FP90 central processor with FP82HT hot stage.

A Bruker 400 NMR was used for NMR data acquisition (Frequency: 400 MHz for ^{1}H-NMR; 100 MHz for ^{13}C-NMR and 376 MHz for ^{19}F-NMR), and the plots were generated by TOPSPIN 2 software (ver. 2.1, Bruker Optics Inc., Billerica, MA, USA) and MestReNova (MNOVA, version-11.3) software.

A Thermo Finnigan Trace – GC 2000 (Thermo Scientific, Austin, TX, USA) and Polaris Q Mass Spectrometer (Thermo Scientific, Austin, TX, USA) were used to follow the reactions and assay product purity. The GC-MS data were collected and processed via Xcalibur software (Ver. 1.4, Thermo Scientific, San Jose, CA, USA).

Differential scanning calorimetry (DSC) analysis was run on a 2920 Modulated DSC from TA instruments (TA Instruments Inc., New Castle, DE, USA). Experimental data was analysed and exported by using the Thermal Advantage software (Version 1.1A, TA Instruments Inc., New Castle, DE, USA).

High Resolution mass spectra were performed by Dr. Dirk Friedrich using an Exactive Plus mass spectrometer (Thermo Scientific, Bremen, Germany). Mass spectra were recorded in the positive ionisation mode with a scan range of 50–700 m/z, a mass resolving power setting of 140,000. To ensure very high mass accuracy, the instrument was mass calibrated daily and a lock mass of m/z 371.10124, due to polysiloxane, was used throughout. The reported compounds were measured as pure solids ionised by electronically excited Helium gas using an ID-cube DART-source (Ionsense, Saugus, MA, USA). Isotopic patterns were simulated using the software Thermo Xcalibur 3.0.63 (Thermo Scientific, Bremen, Germany).

2.1 Representative procedure for aromatic nucleophilic substitution reaction

In a 200 ml round bottom flask was placed hydroxy tail-terminated cyanobiphenyls (10.0 mmol), fluoroarenes (15.0–20.0 mmol, 1.5–2.0 equiv.), dry DMF (15.0–20.0 mL), potassium carbonate (1.38 g, 10.0 mmol, 1.0 equiv.). The resulting suspension was stirred at 40–50° C overnight and the reaction was monitored by TLC analysis. Once complete, water was added dropwise with stirring to fill the flask and then the mixture was extracted with ethyl acetate. The organic layers were washed with water and dried over $MgSO_4$. The product was purified by flash silica column chromatography.

For detailed experimental procedures, see the Supplemental Information.

2.2 Computational methods

All Density Functional Theory (DFT) calculations were performed with Gaussian 09 version D.01 [25]. We employed the M06-2X-D3(SMD = benzonitrile)/def2-TZVP//PBE-D3(SMD = benzonitrile)/def2-SVP level of theory [26–30], similar to our previous studies that calculated dipole moments for mesogenic molecules [7–9]. Our DFT method has been chosen based on benchmark calculations against higher-level computational methods [22] and has proven to yield accurate predictions of mesogen properties including their dipole moments [7–9]. To compute accurate dipole moments, the conformational space of the aliphatic chain of mesogens has to be taken into account because multiple conformer structures are likely to play a role in determining the overall dipole moment of these compounds. Therefore, we generated the conformational modes of the aliphatic chains of mesogens by assuming three different conformations for each C-C and C-O single bonds of the aliphatic chain. Specifically, we considered one anti and two gauche conformations with a starting dihedral angle of 0, 120, and 240 degrees, respectively. From these generated structures, we chose 500 random conformations for each compound to be used in the dipole moment calculations. We limit the conformation space to 500 structures to decrease the computational cost associated with the DFT calculations. Finally, to obtain the conformation-averaged dipole moment for each compound, we calculated the Boltzmann-weighted sum of the dipole moment including each of the 500 structures.

To gain insight into the binding properties of fluorinated aromatic-terminated mesogens to metal salts, which can be relevant for future sensor applications, we performed Binding Free Energy (G_{BE}) calculations at the M06-2X-D3/def2-TZVP//PBE-D3/def2-SVP level of theory. We employed the Neutral Anion Model (NAM), which we have developed to model the interaction between the mesogen and a metal salt [31]. This NAM model has been shown to provide good agreement with experiments, as described in detail in our previous publications [31–33]. We define G_{BE} of mesogens as $G_{BE} = G_{Model+LC} - G_{Model} - G_{LC}$, where $G_{Model+LC}$ is the total free energy of the metal salt cluster model with the bound mesogen, G_{Model} is the free energy of the naked metal-salt cluster model defined in the NAM, and G_{LC} is the free energy of the mesogen molecule in the gas phase. All G_{BE} values were calculated at 298 K and 1 atm. We have found previously that negative G_{BE} values, which indicate strong binding of the mesogens to the metal-salt surfaces, corresponds to homeotropic ordering of mesogens in the bulk LC film, whereas positive G_{BE} suggests the lack of binding and planar ordering [7–9]. To limit computational cost, while still making a fair comparison of the G_{BE} of mesogens, we study only the most stable anti conformation of the aliphatic chain of mesogens in G_{BE} calculations.

3. Synthesis

The parent compound terminated with a pentafluorophenyloxy group (PFC6OCB) was originally described by T. Itahara [10] using a method involving an alkylation between pentafluorophenol and the relevant bromine terminated alkoxyl CB intermediate but the yield was poor (Scheme 2). The Mitsunobu reaction has also been applied to build this fluorinated phenyloxy terminus [34] but overall there are relatively few commercially available highly fluorinated phenols. As a consequence, aromatic nucleophilic substitution (S_NAr) was chosen in our work and this approach often improved the yield. From our previous work [8], 4′-[(6-hydroxy)hexyloxy]-4-cyanobiphenyl had been prepared as an intermediate and here this compound was treated with an excess of hexafluorobenzene in the presence of potassium carbonate (Scheme 2). The desired product of the S_NAr reaction was obtained in good yield without the formation of any byproduct based on NMR data (see SI). This same S_NAr strategy has been utilised for the synthesis of a variety of other derivatives; however, if there are multiple sites for S_NAr reactions to occur then isomeric products may be produced/isolated. In some cases the method of Itahara may be preferred if the relevant phenolic precursor is available and then only a single isomer will be produced.

For the laterally fluorinated derivatives **13–18** found in Table 2, the key laterally fluorinated hydroxycyanobiphenyl intermediates were prepared using a Suzuki reaction of either a fluorinated phenol or a fluorinated cyanophenyl boronic acid (see SI). Interestingly, some of the lateral fluorinated hydroxy tail-terminated cyanobiphenyl intermediates also show nematic properties (see SI).

For the compounds **19–24** shown in Table 3, the tail is connected to the biphenyl as an alkyl group

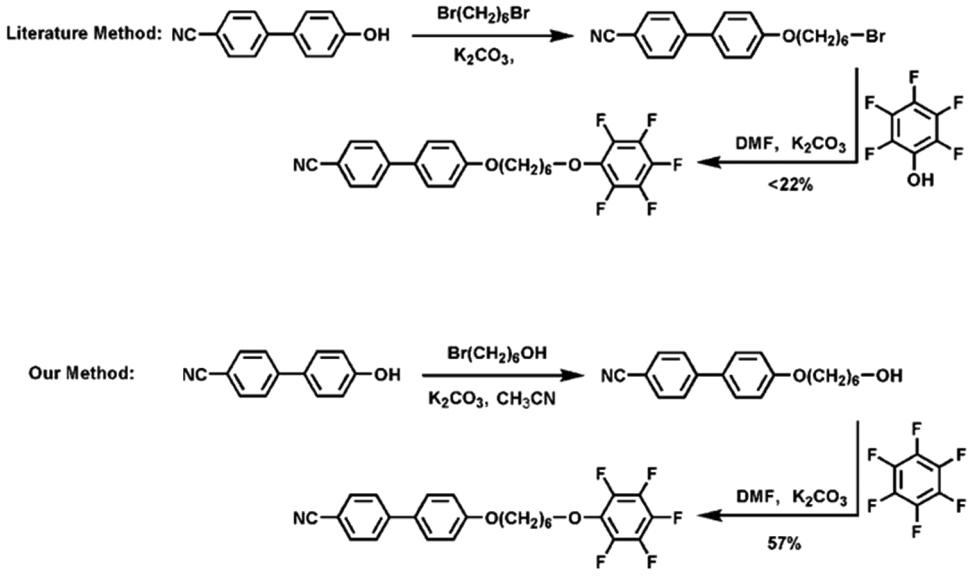

Scheme 2.

Table 2. Phase behaviour of lateral fluorinated derivatives **13**–**18**. (a. no additional phase changes were observed on cooling to −40°C during DSC analysis.).

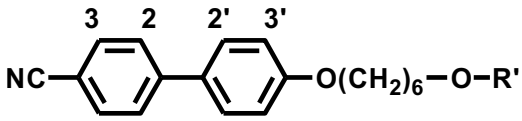

#	Structure	Phase behaviour (°C)
13	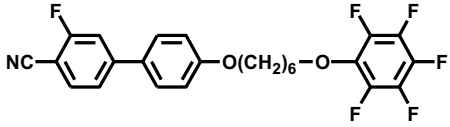	K 54.3 I 17.6 N [a] K 46.6 I 34.3 N − 14.4 K
14	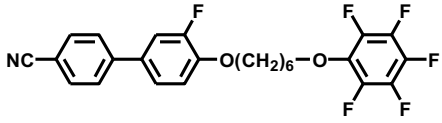	K 38.4 I 20.9 K
15	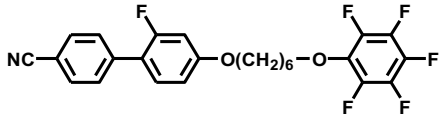	K_1 42.1 K_2 55.2 I 30.2 N [a]
16	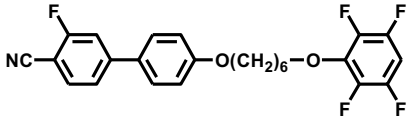	K 53.0 I [a]
17	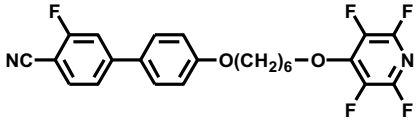	K 67.3 N 69.5 I 68.2 N 61.7 K
18	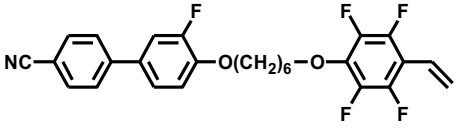	

(no ether linkage) and hydroxy tail-terminated alkylcyanophenyl intermediates are required. Their preparation has been described in our previous work (Scheme 3) [7].

In the case of **27**–**28** incorporating ether connectivity to the biphenyl ring and alkyl connectivity to the halogenated terminating ring were synthesised to compare the mesogenic properties with the alternative mono ether analogues **19**–**24**. Compound **27** was synthesised by following reaction path in Scheme 4, wherein Mitsunobu reaction was performed to obtain the alkyne precursor followed by Sonogashira reaction with pentafluoroiodobenzene and hydrogenation. The analogous compound **28** was synthesised using a different synthetic approach as shown in Scheme 4. In this case, the hydroxy tail-terminated alkylpentafluorophenyl precursor was prepared by Sonogashira reaction and then hydrogenation. Later, the target compound **28** was prepared by Mitsunobu reaction with 4-hydroxy-4′-cyanobiphenyl. In addition, the known dialkoxycyanobiphenyl **26** [10] in Table 3 is synthesised according to the reaction Scheme 2 to better understand its mesogenic properties and to compare with mono alkoxycyanobiphenyl analogue **28**.

Since PFC6OCB (**1**) shows interesting mesogenic properties, the unknown non-fluorinated version PHC6OCB (**25**) was synthesised by Mitsunobu reaction for comparison (see SI). In addition to the above cyanobiphenyl derivatives, two cyano-*p*-terphenyls **29** and **30** were also synthesised. The relevant hydroxy tail-terminated hexyloxy cyano-*p*-terphenyl intermediates were prepared by literature methods (see SI) [31].

All the final products were characterised by NMR spectroscopy (^{1}H, ^{13}C and ^{19}F), and their thermal behaviour examined by Differential Scanning Calorimetry (DSC) and Polarised Optical Microscopy (POM). Generally, the S_NAr reaction shows a high degree of regioselectivity and proceeds cleanly with formation of only para adduct except in the case of target compounds **3, 4, 6** and **16** (see SI). These reactions generated 20%, 17%, 12% and 11% of the respective ortho adducts

Table 3. Phase behaviour of selected fluoroarylyloxy terminated CB derivatives **19**–**24** and **26** with different bridging structure than the compounds in Table 2. (a. Sample never recrystallised in DSC analysis; b. sample recrystallised during the heating cycle).

#	Structure	Phase behaviour (°C)
19	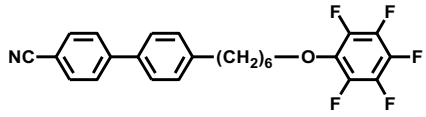	Isotropic. No transitions down to −40
20	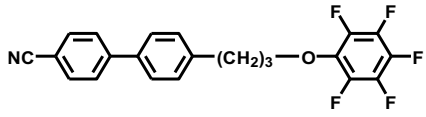	K 57.1 I 33.5 N 9.5 K
21	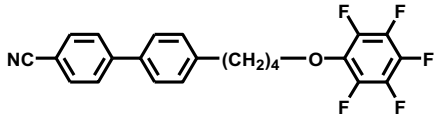	K 47.1 I [a]
22	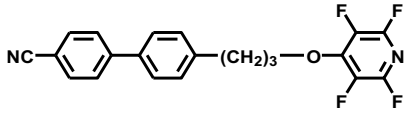	Isotropic. No transitions down to −40
23	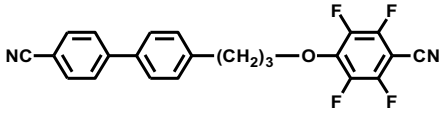	K 104.1 I 70.2 K
24	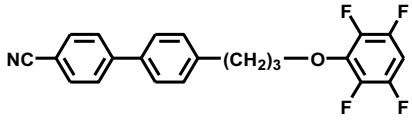	K_1 56.4 K_2 61.24 I 40.9 N − 2.5 K
26	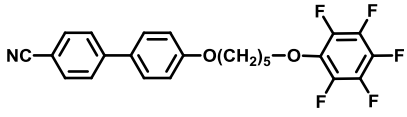	K_1 35.60 K_2 39.63 K_3 44.79 I [b]
PFC5OCB		

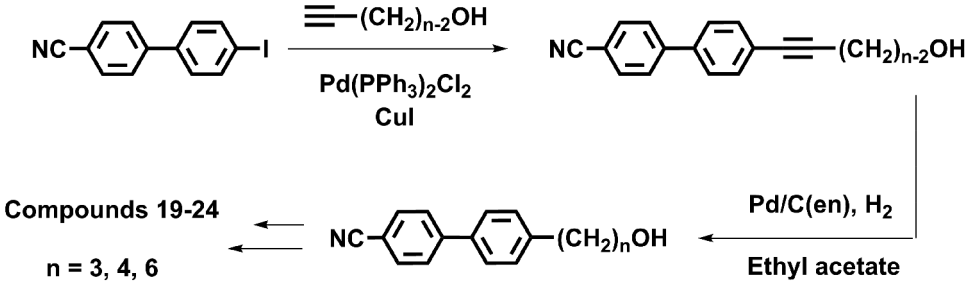

Scheme 3.

(ratios are determined by NMR). It is very difficult to separate these regioisomers and so they have been examined as mixtures. If the pure isomers are needed they might be better prepared using the method of Itahara (and assuming the relevant phenols are available).

4. Results and discussions

The parent compound PFC6OCB (**1**) from Itahara is of particular interest because it exhibits an enantiotropic nematic phase near ambient temperature. In working with this substance we observed that it possess a remarkable supercooling property as seen in Table 1 (DSC shown in

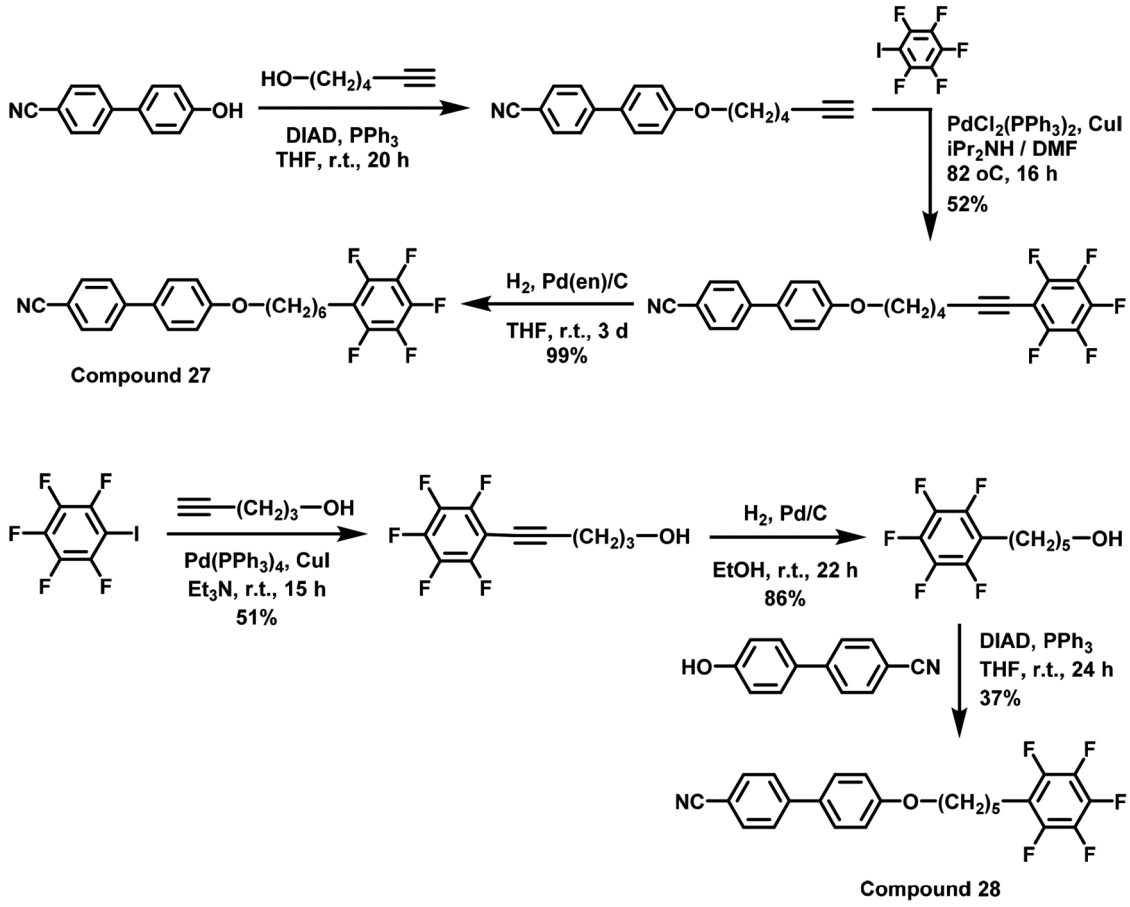

Scheme 4.

SI). Interestingly, the non-fluorinated version, PHC6OCB (**25**), does not show any mesogenic properties at all. The origin of this dramatic contrast of their thermal behaviour remains to be elucidated [35]. In fact, Itahara reported two additional derivatives with a -O(CH_2)$_6$O- spacer, one terminated with 4-fluorophenyl core and the other with a 3,4,5-trifluorophenyl core [10]. These two compounds also possess a nematic phase. Later, K. Kishikawa explained that the π–π interaction between electron-deficient fluorinated ring and the biphenyl moiety may contribute to the stabilisation of nematic phase [36]. In order to study the effect of the pentafluorophenyloxy terminus, we synthesised a series of derivatives with other para-position-functionalised multifluorophenyloxy groups and investigated the thermal behaviour respectively. When the para fluorine atom of the pentafluorophenoxy group was replaced by a H, Cl, Br or nitrile group, only monotropic nematic behaviour is found accompanied by an increase of the clearing points (DSC plot and POM image of compound **2** with a para H atom are shown in Figure 2 (A, B)).

As was noted, in some cases (with Cl and Br groups) the S_NAr reaction used for synthesis gave a mixture of ortho and para adducts which could not be separated and so in these cases the phase behaviour of the mixture is reported. In another case, the presence of a trifluoromethyl at the para-position results in formation of product **5** with a smectic phase instead of a nematic phase. In addition, these derivatives all lose the supercooling property and crystallise relatively readily above room temperature in comparison to PFC6OCB. Interestingly, a vinyl group at para-position leads again to an enantiotropic nematic behaviour but at an elevated temperature range (**7**, Table 1). Compared to the non-fluorinated analogue prepared as polymer precursor by McKeown et al. [15], the perfluorination decreases the nematic phase transition temperature by nearly 40°C.

Still larger fluorinated groups terminating the tail were also prepared and evaluated. Decafluorobiphenyl was examined as an S_NAr substrate and the resulting compound **8** shows monotropic liquid crystal properties with formation of both a nematic and a smectic phase during cooling. Interestingly, compound **9**, which is synthesised from 2,3,4,5,6-pentafluorobiphenyl, also shows monotropic behaviour but here only a nematic phase is observed during cooling. Compound **10** is an analogue of the cyanobiphenyl dimer molecule CBO6OCB [16] but with one perfluorinated phenyl

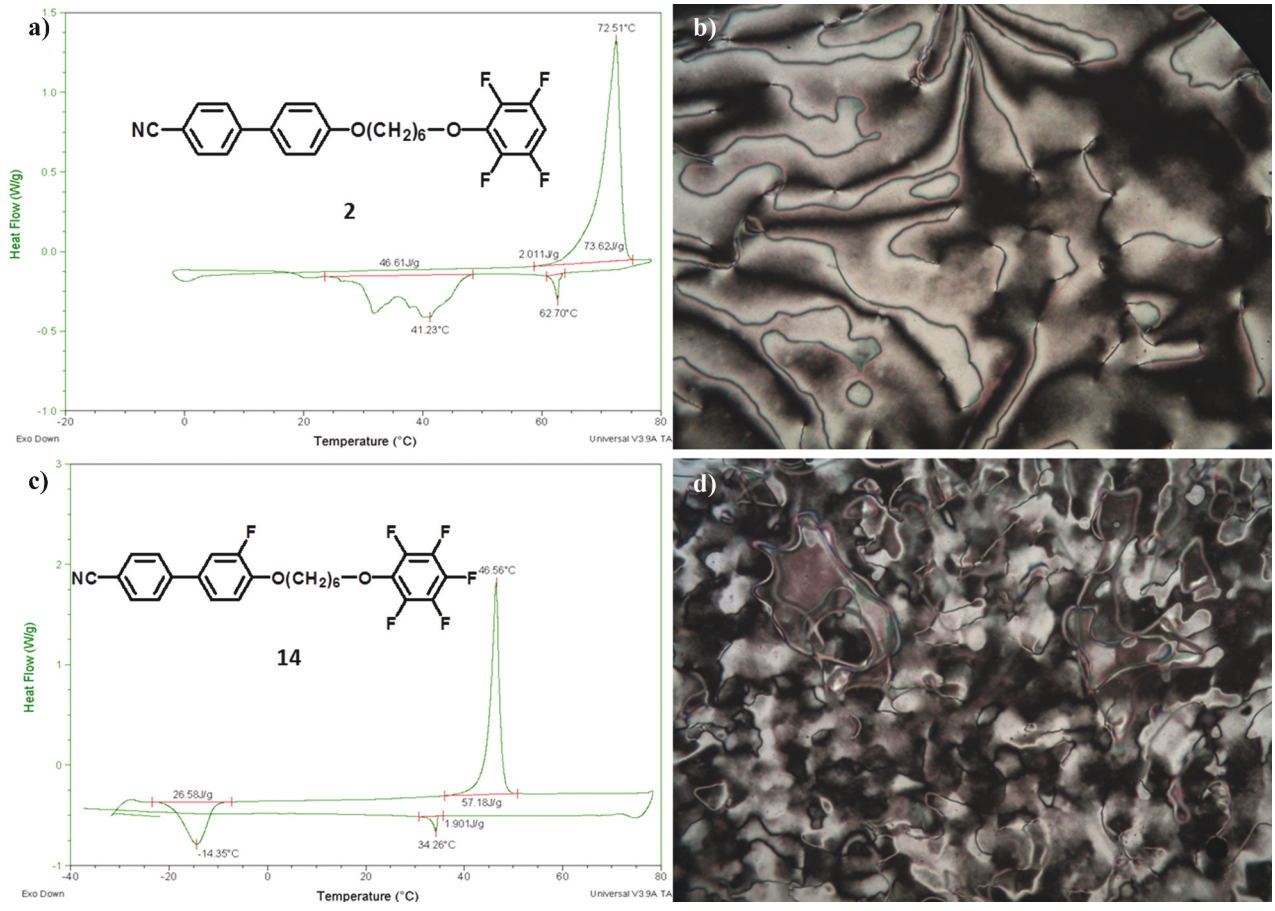

Figure 2. (Colour online) The DSC plot of A) compound 2 (K 72.5 I 63.7 N 41.2 K) and C) compound 14 (K 46.6 I 34.3 N – 14.4 K); Optical microscopy images (crossed-polars) of the nematic phase texture of B) compound 2 at 63°C during the transition from isotropic to nematic phase on cooling and D) compound 14 at 35°C during the transition from isotropic to nematic phase on cooling. (The second cycle is shown for all cases if not mentioned otherwise).

ring. While CBO6OCB shows a nematic phase from 187 to 221°C, compound **10** exhibits only monotropic nematic behaviour and the clearing point was decreased by 60°C due to the fluorination. Compound **11**, prepared from octafluoronaphthalene and bearing a 2-heptafluoronaphthyl terminus, exhibits a similar transition sequence compared to compound **9** and not compound **8**. Another perfluorinated motif— the heterocycle perfluoropyridine (which is also a very important aromatic core for our sensor research involving surface anchoring) was examined and the tetrafluoropyridine terminated derivative **12** possesses a lower clearing point compared to PFC6OCB. This compound shows monotropic nematic below room temperature and some supercooling property as the crystallisation transition was found in the next cycle in DSC analysis. Compared to preliminary results for other terminus and same hexyloxy bridging group, the clearing points are generally higher than the fluorine terminated compound F6OCB, which shows a nematic phase from 61 to 67°C [8], similar to chlorine tail-terminated Cl6OCB [6]. The phase behaviour data for all the compounds just described is summarised in Table 1.

In order to investigate any additional influence of fluorination on the cyanobiphenyl core on the phase behaviour, the lateral fluorinated derivatives as shown in Table 2 were synthesised. We examined fluorine introduction at the 3-, 2′- and 3′-positions (examples with fluorine at the 2-position were not prepared). When the fluorine is located at the 3-position (Entry **13**) or the 3′-position (Entry **14**), the derivatives show monotropic nematic behaviour and supercooling properties while, in contrast, compound **15** with the fluorine at the 2′-position loses all liquid crystal properties and ends up with a lower clearing point than the parent compound. Though monotropic, the nematic phase of compound **14** actually covers the room temperature range as shown in Figure 2 (C, D). Next, different termini were in examined in which lateral fluorination is also present. As a derivative of compound **13**, compound **15**, with one para-fluorine substituted by a hydrogen, shows a monotropic but wider nematic

range above −40°C and also covers ambient temperature. The tetrafluoropyridine terminus (Entry **17**) unfortunately eliminated the mesogenic activity. Compound **18**, which contains a 4-vinyltetrafluorophenyloxy terminus, was synthesised because the analogous compound **7** in Table 1 gives a stable nematic range but surprisingly here, compound **18** shows only a narrow nematic range and the absence of supercooling properties.

The thermal behaviour of these mesogens may also be dramatically influenced by modification of the aliphatic bridging group in addition to core fluorination. All the compounds already described contain a six carbon chain with an ether connection on both ends. In Table 3 derivatives **19**–**24** are presented that differ in carbon chain length and/or ring connectivity. First of all, compounds **19, 20** and **21**, with six (C6CB), three (C3CB) and four (C4CB) carbon chains, respectively, and an alkyl connection to the biphenyl ring, present an odd and even effect as only compound **20** (C3CB) with an odd number of carbons exhibits a monotropic nematic phase as shown in Figure 3 (A, B). Next, several different termini were examined for the C3CB system. The tetrafluoropyridine group (**22**) and 4-cyanotetrafluorophenyloxy group (**23**) failed to bring about any favourable outcome. Compound **22** turns out to be only an isotropic liquid even when cooled down to −40°C while **23** shows only a crystal to isotropic transition. However, the 2,3,5,6-tetrafluorophenyloxy terminus (**24**) exhibits some interesting phase behaviour compared to compound **20** since the monotropic nematic range is wider. Obviously, the full matrix of structure options here has not been explored and likely other compounds with other structure combinations may have useful properties. Moreover, the literature reported dicyanobiphenyl ether-linked compound **26** (PFC5OCB [10]) exhibits no mesogenic properties by DSC and POM, which is inconsistent with the literature reported

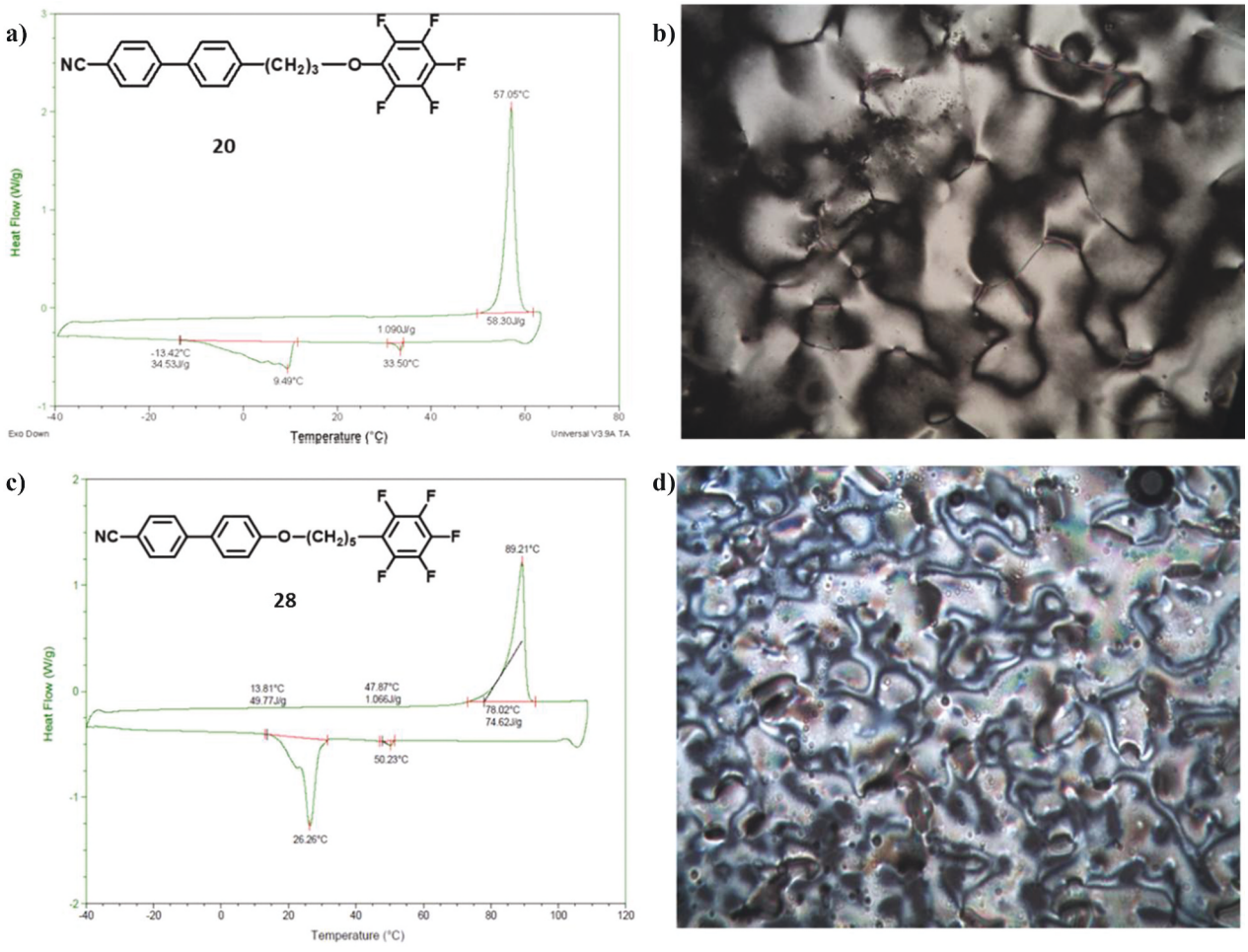

Figure 3. (Colour online) The DSC plot of A) compound 20 (K 57.1 I 33.5 N 9.5 K) and C) compound 28 (K 89.2 I 50.2 N 26.3 K); Optical microscopy images (crossed-polars) of the nematic phase texture of B) compound 20 at 32°C during the transition from isotropic to nematic phase on cooling and D) compound 28 at 51°C during the transition from isotropic to nematic phase on cooling.

result that showed a monotropic nematic phase at 17°C by polarised microscopy. Interestingly, the diether five carbon chain analogue **26** with high polarisability anisotropy exhibits no mesogenic properties, whereas, the monoether five carbon chain analogue **28** (see Table 4) shows a monotropic nematic phase. However, low clearing point and high supercooling properties were observed for analogue **26** compared to analogue **28**.

The mesogenic properties of the compounds analogous to **19–21** but with alternative ring connectivity were also investigated. In the case of compounds **27** and **28** the ether linkage is connected to the biphenyl ring and an alkyl chain with six (C6OCB, **27**) or five (C5OCB, **28**) carbons is connected directly to the pentafluorophenyl ring terminated group as shown in Table 4. The ether linkage to the biphenyl ring analogues were interesting targets due to the extended conjugation of oxygen with the biphenyl core that enhances the polarisability anisotropy.

Like compound **19** (C6CB), the mono cyanobiphenyl ether analogue **27** (C6OCB) with a six carbon chain exhibits no mesogenic properties and remained isotropic until −40°C (but shows high supercooling properties according to DSC). On the other hand, the mono cyanobiphenyl ether analogue **28** (C5OCB) with a five carbon chain showed a monotropic nematic phase as shown in Figure 3 (C, D) with higher clearing point compared to six carbon analogue **27**. The mesogenic property of the monoether analogue **28** (C5OCB) was similar to the mono ether analogue **20** (C3CB) with an odd number of carbon chain.

We have also briefly examined the behaviour of a couple cyanoterphenyls in which the tail is terminated with the pentafluorophenoxy group. The larger version of PFC6OCB (**1**), the terphenyl compound **29** PFC6OCT, shows a wide smectic A phase below a nematic phase and these phases occur at significantly lower temperatures than the analogous terphenyl compounds with no ring termination (6OCT) on the tail as shown in Table 5. In an attempt to further lower the temperature of the nematic phase in this terphenyl, the lateral chlorinated derivative PFC6OClCT (**30**) was prepared and it does have a significantly lower (but narrower) nematic range with supercooling and no smectic phase as shown in Figure 4. As the larger oligophenyls are widely utilised in applications requiring high birefringence, exploitation of the tail termination strategies shown here are relevant [37,38].

Table 4. Phase behaviour of selected multifluorophenyl terminated monoalkoxy cyanobiphenyl derivatives with different bridging groups **27** and **28**. (a. sample did not recrystallise in DSC analysis upon cooling).

#	Structure	Phase behaviour (°C)
27	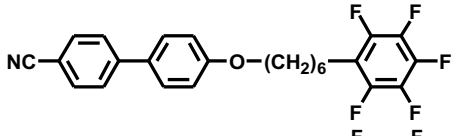	K 76.5 I [a]
28	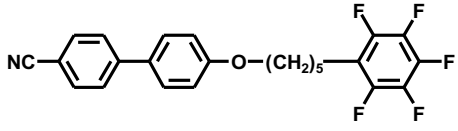	K 89.2 I 50.2 N 26.3 K

Table 5. Phase behaviour of pentafluorophenyloxy terminated alkoxy CT derivatives **29** and **30**. (a. Phase sequence determined by POM) Data available for the analogous parent nonsubsitituted 6OCT is provided for comparison [31].

#	Structure	Phase behaviour (°C)
29	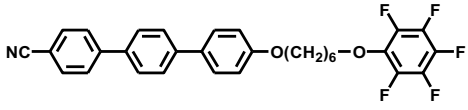	K 117.5 SmA 172.0 N 211.7 I 211.2 N 171.6 SmA 111.3 K[a]
30 PFC6OClCT	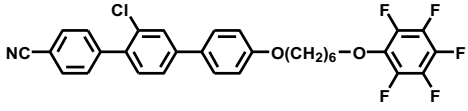	K 93.6 N 112.5 I 111.2 N 59.6 K
6OCT	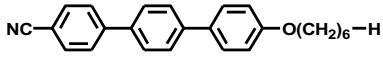	K 90 SmF 115 SmB 169 N 240 I

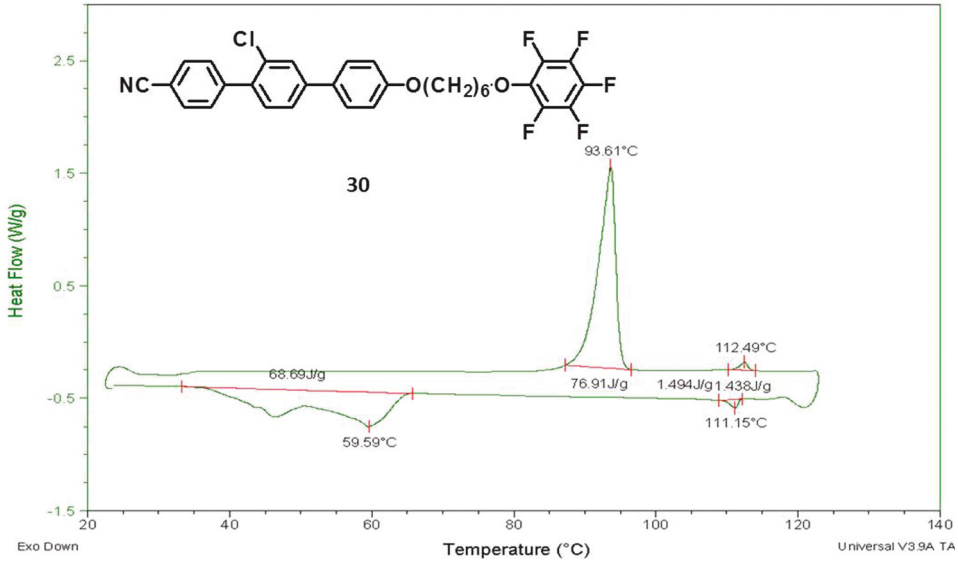

Figure 4. (Colour online) The DSC plot of compound 30 (K 93.6 N 112.5 I 111.2 N 59.6 K).

So far, structural variations of the parent compound PFC6OCB (**1**) with different terminating groups, insertion of lateral aromatic fluorines and different bridging groups were described and it is evident that these modifications have a significant influence on the thermal behaviour. Although most of the behaviour found amongst these materials is not superior to the original PFC6OCB, there are still some promising properties useful for chemoresponsive sensor applications that will require broad nematic phases including ambient temperature. For example, compounds **14, 16, 20, 24** and **28** all show a nematic phase that encompasses ambient temperature and also, to some extent, supercooling which is very useful for applications of liquid crystal mixtures. As a consequence, these compounds were mixed in identical molar ratio (1:1) with PFC6OCB (**1**) to obtain binary mixtures. Amongst these mixtures, the 1:1 mixture of **1** and **24** (which differ by exchange of a single fluorine atom for a hydrogen atom as well as in spacer length and chain connectivity) exhibits the widest enantiotropic nematic phase with the clearing point being 54°C and a nematic phase that persists to at least −40°C based on DSC analysis (see Figure 5 (A, B)). This sample persists in a liquid crystal state for weeks under ambient conditions.

The 1:1 mixture of **1** and **20** (which differ in the length of the spacer and the chain connectivity) also shows a nematic phase from −40 to 50°C (see Figure 5, (C, D)). Similarly, the 1:1 mixtures of **1** and **16** (which differ by core fluorination and tail termination) shows a nematic phase from −40 to 47°C (see Figure 6 (A, B)). In addition, the 1:1 mixture of **1** and **13** (an analogue of **1** with cyanobiphenyl core fluorinated at the 3-position as shown in Table 2) was also examined and shows a nematic phase from −40 to 41°C (see SI for DSC plot). The 1:1 mixture of **1** and **14** (an analogue of **1** with cyanobiphenyl core fluorinated at the 3′-position as shown in Table 2) shows a more narrow nematic phase from −37 to 48°C but also supercools according to DSC analysis, in which the nematic to crystal transition was found on the heating part of the next cycle (see SI for DSC plot). This, in fact, also results in a nematic liquid crystal mixture at ambient temperature for our further study as long as it is stored at room temperature. These samples are currently under examination for chemoresponsive sensor applications. Surely, new promising results may be achieved if the compositions of these binary mixtures are tuned or even if ternary mixtures are made.

Generally, these binary mixtures formed by compounds **13, 14, 16, 20** and **24** respectively with PFC6OCB (**1**) show interesting room temperature nematic phases and these samples stay in a liquid crystal state for weeks under ambient conditions. However, due to the low clearing points possessed by the individual components, the clearing points of the resulting mixtures are relatively close to room temperature, which might hinder their applications. The well known liquid crystal mixture E7 (Merck KGaA, Darmstadt, Germany) contains four components including 8.0% of 4-pentyl-4′-cyanoterphenyl to achieve a higher clearing point [39]. Here we have described the thermotropic nematic mesogen **30** with a relatively high clearing point (112.5°C) and thus it was mixed with PFC6OCB (**1**) in identical molar ratio to get the mixture **PFC6OCB-PFC6OClCT**.

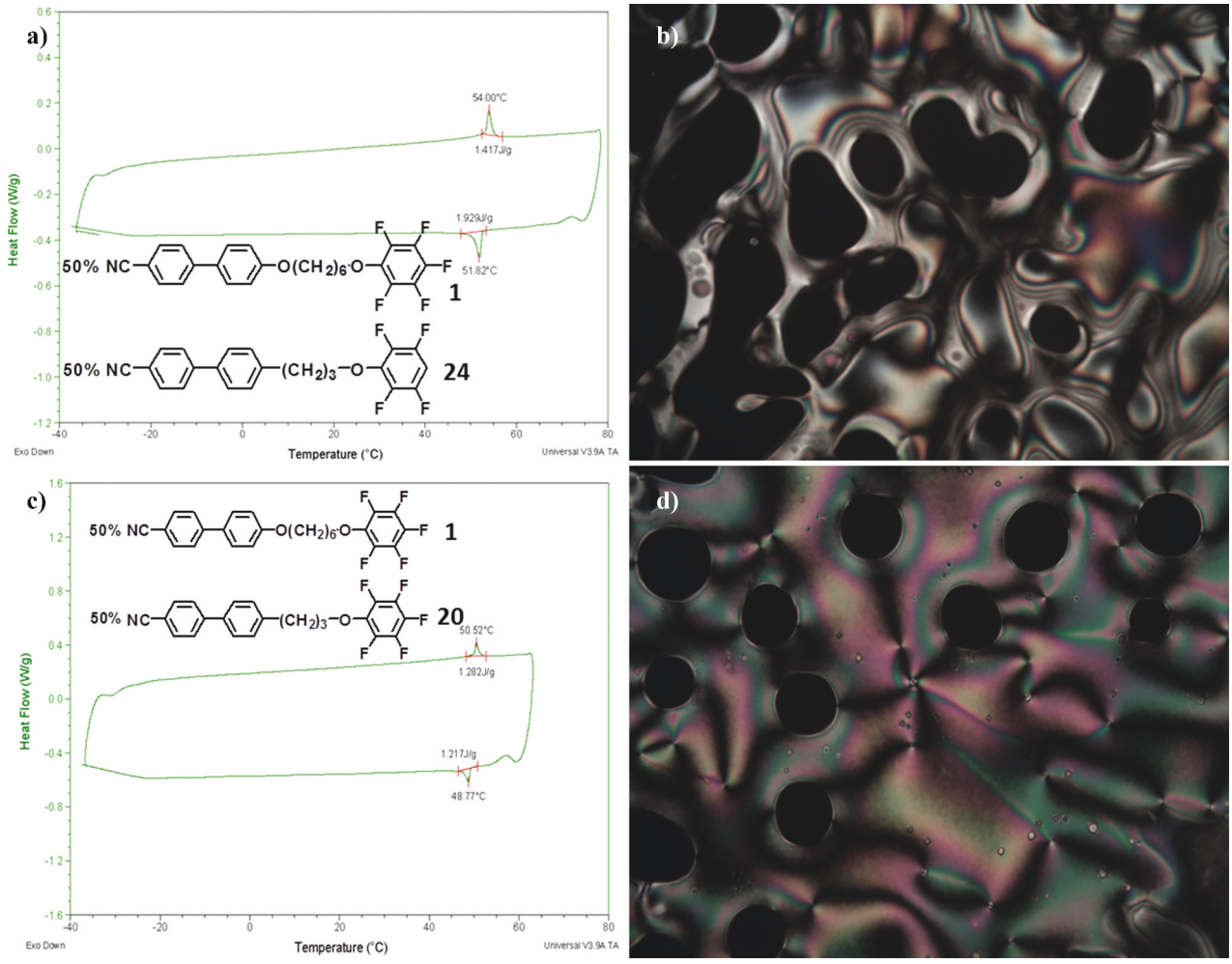

Figure 5. (Colour online) A) The DSC plot of binary mixture by compounds 1 and 24 in equimolar ratio (N 54.0 I 51.8 N) and C) binary mixture by compounds 1 and 20 in equimolar ratio (N 50.5 I 48.8 N); Optical microscopy images (crossed-polars) of the nematic phase texture of B) mixture by 1 and 24 at 54°C during the transition from nematic to isotropic phase on heating and D) mixture by 1 and 20 at 49°C during the transition from isotropic to nematic phase on cooling.

We are delighted to find that a remarkably wide nematic range was obtained up to 87.3°C (see Figure 6 (C, D). In addition, this mixture stays in a liquid crystal state for weeks under ambient conditions. This is a 30°C improvement on the N to I transition compared to the other binary biphenyl mixtures examined thus far.

5. Calculations of dipole moment and binding free energy (G_{BE})

To gain more insight into the effect of the fluorinated aromatic termination on the molecular properties, we calculated the dipole moments of the newly synthesised multifluorophenyloxy terminated C6OCB derivatives **1**–**12** displayed in Table 1. Figure 7 shows the calculated dipole moments of **1**–**12** and detailed results are provided in Table SI.1. We find that the dipole moments of multifluorophenyloxy terminated **1**–**12** are in the range of 9–12 D, which is significantly higher than that of hydrocarbon or hydroxyl-terminated compounds (6–8 D) [7], fluoroalkoxy terminated compounds (7–9 D) [8], and also somewhat higher than that of the range of cyano-terminated compounds (8–10 D) [9] that we have studied previously. For comparison, we have also calculated the dipole moment of **25** in which there is no multifluorophenyloxy termination but only phenyloxy termination. The calculated dipole moment of **25** (8.51 D) indicates that fluorine termination has always increased the dipole moment. Among the multifluorophenyloxy-terminated compounds, the compounds with the highest dipole moment include cyano end group (**6**: 11.11 D; **10**: 11.95 D), whereas the compounds with the lowest dipole moment have hydrocarbon end group (**2**:

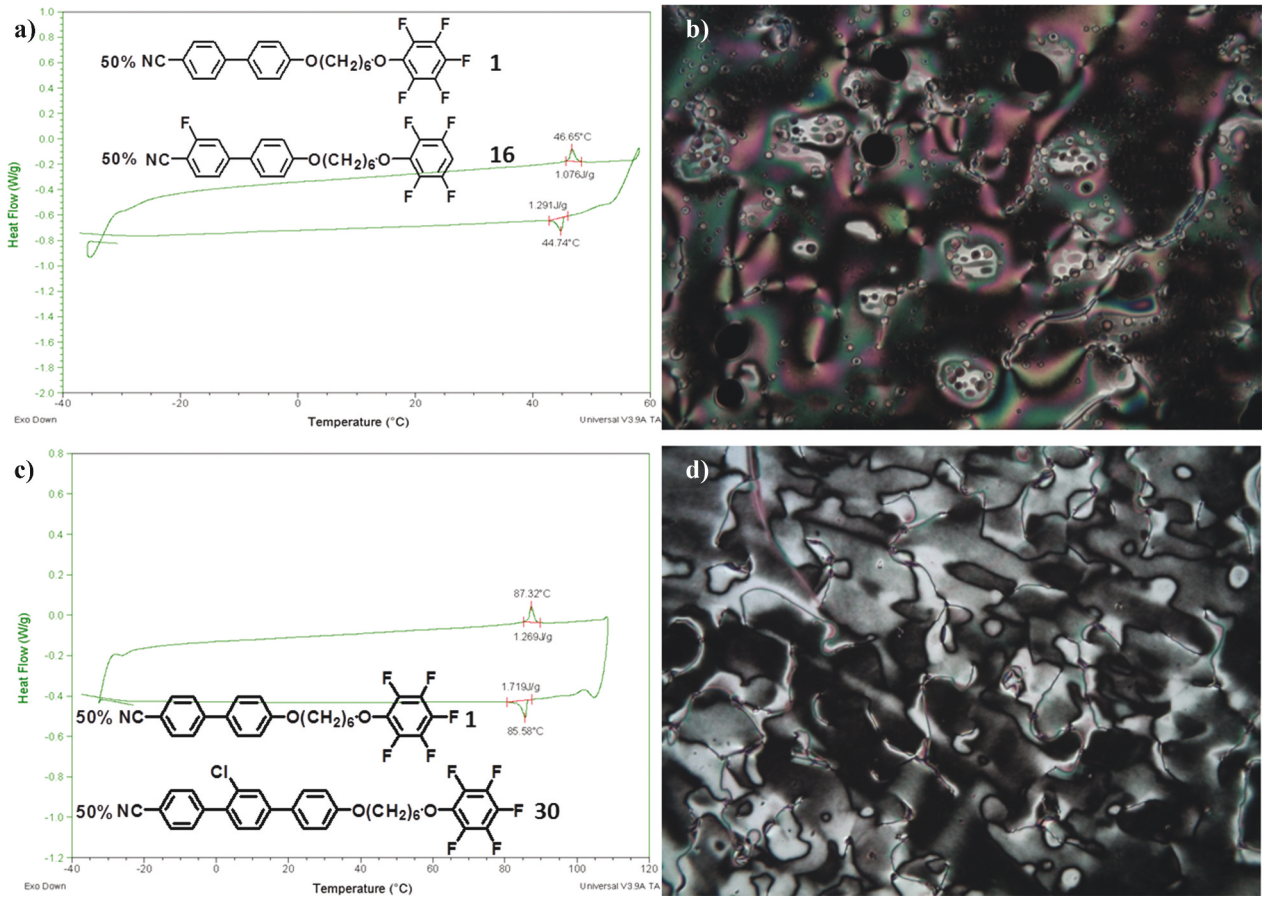

Figure 6. (Colour online) A) The DSC plot of binary mixture by compounds 1 and 16 in equimolar ratio (N 46.7 I 44.7 N) and C) binary mixture PFC6OCB-PFC6OClCT by compounds 1 and 30 in equimolar ratio (N 87.3 I 85.6 N); Optical microscopy images (crossed-polars) of the nematic phase texture of B) mixture by 1 and 16 at 44°C during the transition from nematic to isotropic phase on heating and D) mixture PFC6OCB-PFC6OClCT at 85°C during the transition from isotropic to nematic phase on cooling.

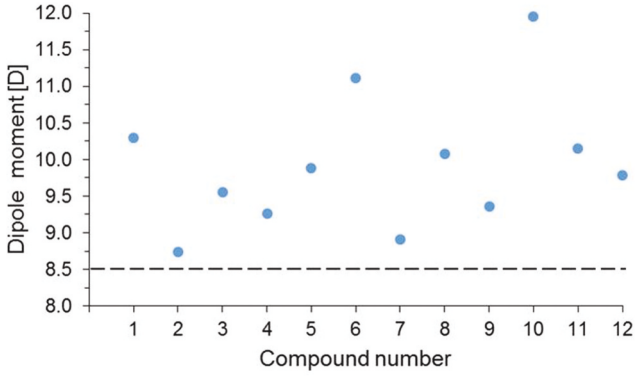

Figure 7. (Colour online) Calculated dipole moments of fluorinated compounds 1–12 in Debye. Structures of 1–12 can be found in Table 1. The dashed line at 8.51 D indicates the dipole moment of parent compound 25 without fluorine termination.

8.74 D; **7**: 8.91 D; **9**: 9.36 D). These results are in agreement with our previous findings that hydrocarbon termination results in the lowest dipole moments, while cyano-termination provides the highest ones [7,9]. The addition of fluorine-containing end groups to the tetrafluorophenyloxy termination provides dipole moments that are in between the previously mentioned compounds with hydrocarbon and cyano end groups (**1**: 10.30 D; **5**: 9.88 D; **8**: 10.08 D; **11**: 10.15 D), which also align well with our previous findings discussed above [8]. Furthermore, we find evidence that increasing electronegativity of the terminating atom can increase the dipole moment of the compound. Compounds **1**–**4** exhibit the same chemical structure except they have F, H, Cl, and Br terminating atoms, respectively. The calculated dipole moments of **1**–**4** are 10.30 D, 8.74 D, 9.55 D, and 9.26 D, respectively, which follows their trend in electronegativity. Finally, we note that the incorporation of the nitrogen into the tetrafluorophenyloxy ring (**12**: 9.79 D) has similar effect on dipole moment as adding additional F-containing groups to the tetrafluorophenyloxy tail such as CF_3 group (**5**: 9.88 D).

To understand more about the interfacial ordering of the fluorinated aromatic-terminated mesogens that are relevant for sensor applications, we calculated the G_{BE}

of **1**–**12** on $Al(ClO_4)_3$, $Ga(ClO_4)_3$, and $Ni(ClO_4)_2$ metal salts (see details in the computational methods section). All calculated results can be found in Table. SI.1. Our previous computational and experimental studies [31] suggested that halogen functional groups cannot bind strongly to metal salts. Therefore, we probed all functional groups at both tails except halogens to find the strongest binding functional group in all compounds. We found that the cyanobiphenyl tail binds considerably stronger than other functional groups. This is still true when there is a second cyano group at the multifluorophenyloxy tail. Previously, we have established that fluorine modification of the cyanobiphenyl tail decreases the binding strength to metal-salt surfaces [31]. Therefore, we think that the weak binding of the cyano group at the multifluorophenyloxy tail is the consequence of the effect of the proximity of fluorine atoms. The cyano group is directly attached to the tetrafluorophenyloxy group in **6**, whereas there is a phenyl linker between the two in **10**; this can explain why we find 0.30 eV difference in G_{BE} between the head and the tail in **6** to $Al(ClO_4)_3$, while there is only 0.08 eV difference in G_{BE} for **10**. We note here that 0.06 eV difference in G_{BE} at room temperature results in one order of magnitude difference in equilibrium constant; thus, the 0.08 eV difference still indicates the dominance of the cyanobiphenyl tail on the surface. Finally, we mention that fluorinated pyridine tail binds 0.49 eV weaker to $Al(ClO_4)_3$ than the cyanobiphenyl tail in **12**. Our previous experimental and computational analyses have shown that a pyridine functional group can bind stronger to metal salt surfaces than a cyanobiphenyl group [31–33], which indicates the significant effect of the fluorination of the pyridine ring on binding strength.

We further analyse the change in G_{BE} with different compounds (**1**–**12**). We find that G_{BE} for the same metal salt does not show any change within 0.02 eV between **1**–**12**. This result is consistent with our previous findings for hydroxyl, fluorine, and cyano-terminated mesogens suggesting that if there is long enough alkyl chain (3–4 CH_2 groups) between the two tails, modifications of one tail do not impact considerably the binding strength of the other tail [7–9].

Finally, we compare the G_{BE} of **1**–**12** on different metal salts. As mentioned above, we find that all compounds bind similarly to the same metal salt, which is also consistent with our previously established practice that PhCN is an adequate surrogate molecule to model compounds with cyanobiphenyl tail [v]. We do see, however, difference between the G_{BE} of mesogens related to different metal salts. G_{BE} of **1**–**12** is −0.52 eV, −0.66 eV, and −1.10 eV for $Al(ClO_4)_3$, $Ga(ClO_4)_3$, and $Ni(ClO_4)_2$ metal salts, respectively, which is similar to what we have found for fluorine or cyano terminated mesogens [8,9]. Based on previous results [31–33], negative G_{BE} predicts homeotropic alignment at the mesogen-metal salt interface; therefore, all of these compounds are suggested to assume homeotropic orientation in experiments in contact with $Al(ClO_4)_3$, $Ga(ClO_4)_3$, and $Ni(ClO_4)_2$ metal salts.

To evaluate the above-described calculated binding free energy and predicted LC anchoring on metal salt-decorated surfaces, we characterised the anchoring of compound **1** when it is sandwiched between two metal

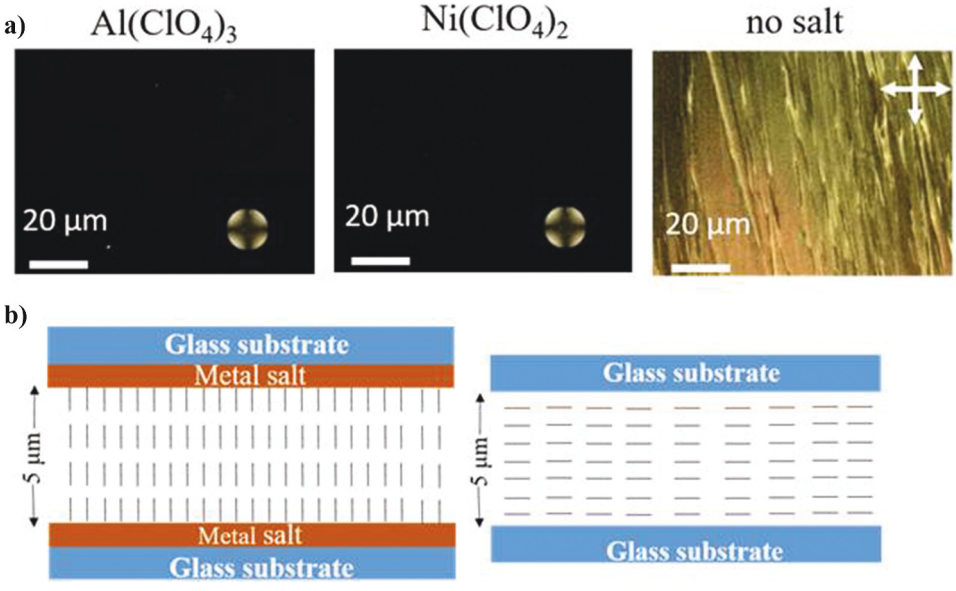

Figure 8. (Colour online) A) Cross-polarised images of compound 1 confined between two galls surfaces decorated with and without metal salt coating. Metal salt coating: Al(ClO4)3 and Ni(ClO4)2 with the surface density of ~15 pmol/mm2. B) Schematic illustration of the experimental setup and director profile of compound 1 when it adopts homrotropic orientation on metal salts and planar orientation on bare glass.

salt-decorated glass interfaces (details in SI). The surface densities of coated metal cations are ~15 pmol/mm^2, which is sufficient to obtain more than 1 ML metal salts coverage as confirmed in our past study [32]. As shown in Figure 8 (A, B), compound **1** adopted homeotropic (perpendicular) orientation on $Al(ClO_4)_3$ and $Ni(ClO_4)_2$ (dark image between crossed polarisers). This observation is consistent with the computational prediction of strong binding of the cyano group of PhCN to Al^{3+} cation (−0.52 eV in Table SI.1) and Ni^{2+} cation (−1.10 eV in Table SI.1) as discussed earlier. As a control experiment, we observed compound **1** adopted non-homeotropic (tilted or planar) orientation on bare glass surface without metal-salt coating as shown in Figure 8.

6. Conclusion

In this work, a series of 4-alkoxy-4′-cyanobiphenyl and 4-alkyl-4′-cyanobiphenyl derivatives bearing a variety of fluorinated aromatic termini were mostly synthesised via a simple S_NAr reaction and their thermal behaviour was investigated. Structural variations including insertion of aromatic lateral fluorine and tailoring of the bridging group have made dramatic influence on the liquid crystal properties. Compounds **13, 14, 16, 20, 24** and **28** show a nematic phase close to ambient temperature as well as supercooling properties and the binary mixtures made with PFC6OCB (**1**) in identical molar ratio show relatively wide nematic ranges while the mixture **PFC6OCB-PFC6OClCT**, which is made by PFC6OCB (**1**) and lateral chlorinated cyanoterphenyl compound **30** in identical molar ratio exhibit a remarkably wide nematic phase. We also calculated the dipole moments of **1**–**12** and their G_{BE} on $Al(ClO_4)_3$, $Ga(ClO_4)_3$, and $Ni(ClO_4)_2$ metal salts. We believe the fluorinated aryloxy terminated molecules tend to assume homeotropic orientation on these metal salt surfaces, which is confirmed by examination of compound **1** on $Al(ClO_4)_3$ and $Ni(ClO_4)_2$ decorated surfaces. Their application in anchoring transitions will be described in separate paper.

Acknowledgments

This work was supported by the National Science Foundation (DMREF grant: DMR-1921668, DMR-1921696, and DMR-1921722). Part of the computational work conducted by T. S., J.G. and M.M. in this study was carried out at various external computational resource facilities through the DoD High Performance Computing Modernization Program (US Air Force Research Laboratory DoD Supercomputing Resource Center (AFRL DSRC), the US Army Engineer Research and Development Center (ERDC), and the Navy DoD Supercomputing Resource Center (Navy DSRC), grant number: ARONC43623362), all supported by the Department of Defense.

Disclosure statement

No potential conflict of interest was reported by the author(s).

Funding

This work was supported by National Science Foundation [1921668, 1921696 and 1921722].

References

[1] Gray GW, Harrison KJ, Nash JA. New family of nematic liquid crystals for displays. Electron Lett. 1973;9(6):130–131.
[2] Chan LKM, Gray GW, Lacey D. Synthesis and evaluation of some 4,4″-disubstituted lateral fluoro-1,1′:4,1″-terphenyls. Mol Cryst Liq Cryst. 1985;123(1–4):185–204.
[3] Gray GW, Hird M, Toyne KJ. The synthesis and transition temperatures of some lateral monofluoro-substituted 4,4″-dialkyl- and 4,4″-alkoxyalkyl-1,1′:4′,1″-terphenyls. Mol Cryst Liq Cryst. 1991;195(1):221–237.
[4] Gray GW, Hird M, Lacey D, et al. The synthesis and transition temperatures of some 4,4”-dialkyl- and 4,4”-alkoxyalkyl-1,1′:4′,1”-terphenyls with 2,3- or 2′,3′-difluoro substituents and of their biphenyl analogs. J Chem Soc Perkin Trans 2. 1989;(12):2041–2053. DOI:10.1039/P29890002041.
[5] Aziz N, Kelly SM, Duffy W, et al. Rod-shaped dopants for flexoelectric nematic mixtures. Liq Cryst. 2009;36(5):503–520.
[6] Davis EJ, Mandle RJ, Russell BK, et al. Liquid-crystalline structure–property relationships in halogen-terminated derivatives of cyanobiphenyl. Liq Cryst. 2014;41(11):1635–1646.
[7] Wang K, Jirka M, Rai P, et al. Synthesis and properties of hydroxy tail terminated cyanobiphenyl liquid crystals. Liq Cryst. 2019;46(3):397–407.
[8] Wang K, Rai P, Fernando A, et al. Synthesis and properties of fluorine tail-terminated cyanobiphenyls and terphenyls for chemoresponsive liquid crystals. Liq Cryst. 2020;47(1):3–16.
[9] Wang K, Szilvási T, Gold JI, et al. New room temperature nematogens by cyano tail termination of alkoxy and alkyl-cyanobiphenyls and their anchoring behavior on metal salt-decorated surface. Liq Cryst. 2020;47(4):540–556.
[10] Itahara T. Effect of the pentafluorophenyloxy group on liquid crystalline behaviour. Liq Cryst. 2005;32(1):115–118.
[11] Imrie CT, Henderson PA. Liquid crystal dimers and higher oligomers: between monomers and polymers. Chem Soc Rev. 2007;36(12):2096–2124.
[12] Mandle RJ, Davis EJ, Voll -C-CA, et al. Self-organisation through size-exclusion in soft materials. J Mater Chem C. 2015;3(10):2380–2388.
[13] Kim D-J, Oh N-K, Lee M, et al. Liquid crystalline assembly of calamatic mesogens and rod-coil molecule

by Pd and Ru complexation. Mol Cryst Liq Cryst. 1996;280(1):129–134.
[14] Cook A, Badriya S, Greenfield S, et al. Styrene-containing mesogens. Part 1: photopolymerisable nematic liquid crystals. J Mater Chem. 2002;12(9):2675–2683.
[15] McKeown NB, Cook A. A novel series of styrene-based liquid crystal monomers displaying either nematic or chiral nematic phases. Liq Cryst. 2006;33(9):1021–1026.
[16] Emsley JW, Luckhurst GR, Shilstone GN, et al. The preparation and properties of the α,ω-bis(4,4-cyanobiphenyloxy)alkanes: nematogenic molecules with a flexible core. Mol Cryst Liq Cryst. 1984;102(8–9):223–233.
[17] Cestari M, Diez-Berart S, Dunmur DA, et al. Phase behavior and properties of the liquid-crystal dimer 1,7-bis(4-cyanobiphenyl-4-yl) heptane: A twist-bend nematic liquid crystal. Phys Rev E. 2011;84(3–1):031704.
[18] Sebastián N, López DO, Robles-Hernández B, et al. Dielectric, calorimetric and mesophase properties of 1′′-(2′,4-difluorobiphenyl-4′-yloxy)-9′′-(4-cyanobiphenyl-4′-yloxy) nonane: an odd liquid crystal dimer with a monotropic mesophase having the characteristics of a twist-bend nematic phase. Phys Chem Chem Phys. 2014;16(39):21391–21406.
[19] Paterson DA, Abberley JP, Harrison WTA, et al. Cyanobiphenyl-based liquid crystal dimers and the twist-bend nematic phase. Liq Cryst. 2017;44:127–146.
[20] Paterson DA, Gao M, Kim YK, et al. Understanding the twist-bend nematic phase: the characterisation of 1-(4-cyanobiphenyl-4′-yloxy)-6-(4-cyanobiphenyl-4′-yl)hexane (CB6OCB) and comparison with CB7CB. Soft Matter. 2016;12(32):6827–6840.
[21] Nayani K, Rai P, Bao N, et al. Liquid crystals withinterfacial ordering that enhances responsiveness tochemical targets. Adv Mater. 2018;30(27):1706707/1–1706707/7.
[22] Szilvási T, Roling LT, Yu H, et al. Design of chemoresponsive liquid crystals through integration of computational chemistry and experimental studies. Chem Mater. 2017;29(8):3563–3571.
[23] Katagiri T, Ota S, Ohira T, et al. Synthesis of thiophene/phenylene co-oligomers. V. Functionalization at molecular terminals toward optoelectronic device applications. J Hetero Chem. 2007;44(4):853–862.
[24] Sajiki H, Hattori K, Hirota K. The formation of a novel Pd/C–ethylenediamine complex catalyst: chemoselective hydrogenation without deprotection of the O-benzyl and N-Cbz groups. J Org Chem. 1998;63(22):7990–7992.
[25] Frisch MJ, Trucks GW, Schlegel HB, et al. Gaussian 09, revision D.01. Wallingford CT: Gaussian, Inc.; 2009.
[26] Perdew JP, Burke K, Ernzerhof M. Generalized gradient approximation made simple. Phys Rev Lett. 1996;77(18):3865–3868.
[27] Weigend F, Ahlrichs R. Balanced basis sets of split valence, triple zeta valence and quadruple zeta valence quality for H to Rn: design and assessment of accuracy. Phys Chem Chem Phys. 2005;7(18):3297–3305.
[28] Zhao Y, Truhlar DG. The M06 suite of density functionals for main group thermochemistry, thermochemical kinetics, noncovalent interactions, excited states, and transition elements: two new functionals and systematic testing of four M06-class functionals and 12 other functionals. Theor Chem Acc. 2008;120(1–3):215–241.
[29] Marenich AV, Cramer CJ, Truhlar DG. Universal solvation model based on solute electron density and on a continuum model of the solvent defined by the bulk dielectric constant and atomic surface tensions. J Phys Chem B. 2009;113(18):6378–6396.
[30] Grimme S, Antony J, Ehrlich S, et al. A consistent and accurate ab initio parametrization of density functional dispersion correction (DFT-D) for the 94 elements H-Pu. J Chem Phys. 2010;132(15):154104/1–154104/19.
[31] Yu H, Szilvási T, Rai P, et al. Computational chemistry-guided design of selective chemoresponsive liquid crystals using pyridine and pyrimidine functional groups. Adv Funct Mater. 2018;28(13):1703581/1–-1703581/10.
[32] Szilvási T, Bao N, Yu H, et al. The role of anions in adsorbate-induced anchoring transitions of liquid crystals on surfaces with discrete cation binding sites. Soft Matter. 2018;14(5):797–805.
[33] Szilvási T, Bao N, Nayani K, et al. Redox-triggered orientational responses of liquid crystals to chlorine gas. Angew Chem Int Ed. 2018;57(31):9665–9669.
[34] Lee MT, Goodstein MB, Lalic G. Synthesis of isomerically pure (z)-alkenes from terminal alkynes and terminal alkenes: silver-catalyzed hydroalkylation of alkynes. J Am Chem Soc. 2019;141(43):17086–17091.
[35] Zang Z, Zhang D, Wan X, et al. The synthesis and property of liquid crystalline 4-alkoxyl-4″-cyano-p-terphenyls. Mol Cryst Liq Cryst. 2000;339(1):145–158.
[36] Kishikawa K. Utilization of the perfluoroarene-arene interaction for stabilization of liquid crystal phases. Isr J Chem. 2012;52(10):800–808.
[37] Peng FL, Chen Y, Wu S-T, et al. Low loss liquid crystals for infrared applications. Liq Cryst. 2014;41(11):1452–1545.
[38] Peng FL, Chen HW, Tripathi S, et al. Fast response infrared phase modulator based on polymer network liquid crystal. Opt Mater Express. 2015;5(2):265–273.
[39] Mouquinho A, Saavedra M, Maiau A, et al. Films based on new methacrylate monomers: synthesis, characterisation and electro-optical properties. Mol Cryst Liq Cryst. 2011;542(1):132/[654] –140/[662].